

# RefineLoc: Iterative Refinement for Weakly-Supervised Action Localization

Humam Alwassel<sup>1\*</sup> Alejandro Pardo<sup>1\*</sup> Fabian Caba Heilbron<sup>2</sup> Ali Thabet<sup>1</sup> Bernard Ghanem<sup>1</sup>  
<sup>1</sup>King Abdullah University of Science and Technology (KAUST) <sup>2</sup>Adobe Research  
 {humam.alwassel, alejandro.pardo, ali.thabet, bernard.ghanem}@kaust.edu.sa caba@adobe.com

## Abstract

Video action detectors are usually trained using datasets with fully-supervised temporal annotations. Building such datasets is an expensive task. To alleviate this problem, recent methods have tried to leverage weak labelling, where videos are untrimmed and only a video-level label is available. In this paper, we propose RefineLoc, a new weakly-supervised temporal action localization method. RefineLoc uses an iterative refinement approach by estimating and training on snippet-level pseudo ground truth at every iteration. We show the benefit of this iterative approach and present an extensive analysis of different pseudo ground truth generators. We show the effectiveness of our model on two standard action datasets, ActivityNet v1.2 and THUMOS14. RefineLoc equipped with a segment prediction-based pseudo ground truth generator improves the state-of-the-art in weakly-supervised temporal localization on the challenging and large-scale ActivityNet dataset by 1.5%.

## 1. Introduction

Weak supervision has emerged as an effective way to train computer vision models using labels that are easy and cheap to acquire. This training strategy is particularly relevant for video tasks, where data collection and annotation costs are prohibitively expensive. In this paper, our goal is to localize actions in time when no information about the start and end times of these actions is available (neither in training nor test). The lack of temporal supervision makes it challenging to train models that discriminate between action and background segments. Current methods for weakly-supervised temporal action localization focus on either learning a Class Activation Map by using soft-attention [58], regularizing attention with an L1 loss [37], or leveraging Co-Activity and Multiple Instance Learning losses [42]. Alternatively, Shou *et al.* [49] and Liu *et al.* [33] focus on generating temporal boundaries using priors such as those encouraged by contrastive losses. All previ-

\*indicates equal contribution.

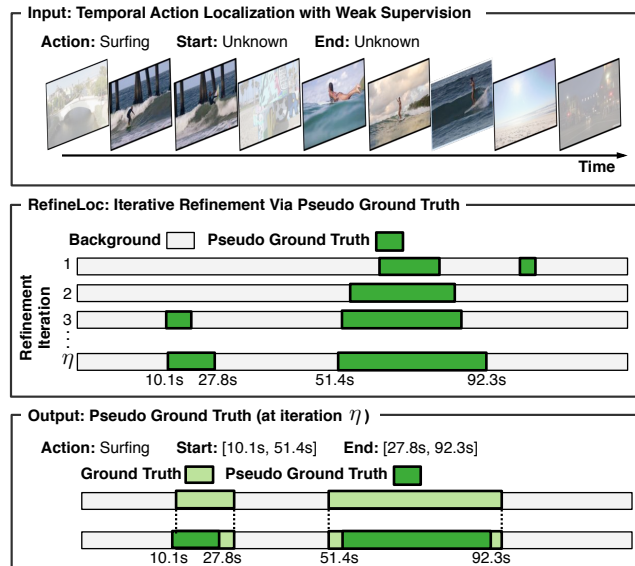


Figure 1: **Iterative Refinement for Weak Supervision.** We summarize the pseudo ground truth generation strategy used by RefineLoc. *Top:* The input is an untrimmed video, where only a video-level label (Surfing) is available; our goal is to correctly localize actions in time. *Middle:* RefineLoc aims to approximate the true foreground-background labels through iteratively generating pseudo ground truth (dark green boxes) using information from a weakly-supervised model. Our key idea is to use the pseudo ground truth from iteration  $\eta - 1$  to supervise the detection model at iteration  $\eta$ . *Bottom:* The pseudo ground truth of iteration  $\eta$  (dark green) closely approximates the actual ground truth (light green).

ous methods provide elegant strategies to localize actions in a weakly-supervised manner; however, they are all trained in a single shot and disregard all temporal cues. As a result, their performance lags far behind that of fully-supervised methods trained on temporal action annotations.

In the object detection scenario, it has been shown that refining a detection network using pseudo ground truth considerably reduces the performance gap between fully and weakly-supervised object detectors [55, 66]. Such pseudo ground truth refers to a set of sampled object predictions

from a weakly-supervised model, which are assumed as actual object locations in a next refinement iteration. Despite their success in the object detection domain, these methods are not directly applicable to temporal action localization. We argue this is in part due to the lack of reliable *unsupervised* region proposals as it is the case in object detection.

In this paper, we propose RefineLoc, a weakly-supervised temporal action localization method, which incorporates an iterative refinement strategy by leveraging pseudo ground truth. Figure 1 shows an example of the iterative refinement process RefineLoc employs via pseudo ground truth generation. Contrary to object detection methods, we build our refinement strategy to operate over snippet-level attention and classification modules, making it suitable for temporal localization. The intuition behind iterative refinement is to leverage a weakly-supervised model which captures decent temporal information about actions to annotate snippets with foreground (action) and background (no action) as pseudo labels. This pseudo ground truth can then be used to train the snippet-level attention module in a supervised manner. Although such pseudo labels are noisy, it has been shown that neural networks are reasonably robust against such label perturbations [46]. To avoid bias towards learning from easy examples, we randomly maintain a fixed pseudo ground truth ratio. Our studies of multiple pseudo ground truth generators show that our best configuration outperforms the state-of-the-art.

**Contributions:** We summarize our contributions as 2-fold. (1) We introduce RefineLoc, an iterative refinement model for weakly-supervised temporal action localization. The model is crafted to leverage snippet-level pseudo ground truth to improve its performance over training iterations. (2) We observe that RefineLoc improves the state-of-the-art in ActivityNet by 1.5%, and this improvement is a direct result of the proposed iterative refinement strategy.<sup>1</sup>

## 2. Related Work

**Action Recognition.** The advent of action recognition datasets such as UCF-101 [54], Sports-1M [25], and Kinetics [26] has fueled the development of accurate action recognition models. Traditional approaches include extracting hand-crafted representations aimed at capturing spatiotemporal features [29, 57]; however, nowadays deep learning based approaches are more attractive due to their high capacity. Take for instance the work of Simonyan and Zisserman [52], which proposed to encode spatial and temporal information with Convolutional Neural Networks. Their two-stream model represents appearance with RGB frames and motion with stacked optical flow vectors, which combined outperformed traditional hand-crafted represen-

tations. However, the two-stream model encodes each frame independently neglecting mid-level temporal information. To overcome this drawback, Wang *et al.* introduced the Temporal Segment Network (TSN) [59], an end-to-end framework that captures long-term temporal information. TSN along with other recent architectures (*e.g.* I3D [9] and C3D [56]) have become the *de facto* video representation backbones for temporal action localization [43], action segmentation [18], and event captioning [61].

**Fully-supervised Temporal Action Localization.** Multiple strategies have been developed for temporal action localization with full-supervision available at training time [13, 19, 21, 48, 63]. The first set of approaches used sliding windows combined with complex activity classifiers to detect actions in time [17, 39]. These methods paved the way for this type of research, and established baselines and a reference for the difficulty of the problem. However, they manifested limitations regarding their runtime complexity. The second generation of methods used action proposals to speed up the search process [4, 5, 20, 32, 50]. These temporal proposals are generated quickly, and their goal is to narrow down the number of candidate segments the action classifier examines. A third generation and current state-of-the-art approaches learn action proposals and action classifiers jointly, while back-propagating through the video representation backbone [11, 60, 67]. Across these generations of approaches, not only has accuracy significantly improved but so has runtime; however, all methods still rely on strong supervision, which is prohibitively expensive to acquire.

**Weakly-supervised Temporal Action Localization.** The challenge in this task is to learn to discriminate between background and action segments without having explicit temporal training samples, but instead, only a coarse video-level supervision signal. Hide-and-seek [28] embraces this quest by randomly hiding video regions to encourage their model to discover discriminative parts, which they find correlating with action segments. Wang *et al.* [58] introduced UntrimmedNets, which only use video-level annotations to perform temporal localization. This method uses TSN [59] as a backbone and learns a soft-attention layer to focus on snippets that boost the video classification performance the most. Similarly, the Spatiotemporal Pooling Network of Nguyen *et al.* [37] stacks an attention layer regularized with an L1 loss. This follows the intuition that only a sparse number of video snippets are action segments. Another recent alternative is W-TALC [42], where a co-activity loss is combined with a multiple instance learning loss to boost detection performance. A group of methods including AutoLoc [49] and CleanNet [33] learn to generate action proposals in an unsupervised way using contrast cues among action classification predictions. With the end goal of addressing the lack of temporal information, other works have innovated strategies such as incorporating temporal

<sup>1</sup>To enable reproducibility and promote future research, we will release the source code, models, and benchmark results for this paper.

structure [64], modeling background [38], or using external knowledge (e.g. action count [35]). All previous approaches have paved the way for achieving accurate temporal localization without strong supervision. Our work builds upon these ideas and complements them with a key insight: leveraging pseudo labels while *iteratively* training the model.

### Weak Supervision and Pseudo-labelling in Vision Tasks.

Weak supervision has been widely studied in other vision tasks such as object detection [2, 40, 47, 53], semantic segmentation [41, 62], or other video tasks [16, 22, 23, 44]. For video tasks, a variety of weak supervision cues have been used including movie scripts [15, 27, 30, 34], action ordering priors [3, 10, 14, 45], and different levels of supervision [12]. These video related solutions have proposed innovative ways to reduce labelling expense; however, they still require laborious annotations (action spots) or privileged information (such as transcripts), which are difficult to obtain beyond controlled settings. Concerning pseudo-labelling, it has been used, for instance, to design state-of-the-art methods for weakly-supervised object detection [55, 66], train image classification backbones [7, 8], and build pose detectors [36]. These works have inspired our model, which addresses challenges unique to the weakly supervised temporal action localization task, namely the presence of only a sparse supervision signal (video-level action category) and of highly similar context surrounding the action [1].

## 3. RefineLoc

In this section, we discuss the details of our RefineLoc architecture, the pseudo ground truth label generation, and the iterative refinement process. The input to our model is an untrimmed video and the expected output is a set of action segment predictions. RefineLoc is supervised on weak labels (*i.e.* video-level action labels) and **does not use** any temporal annotations of action instances. RefineLoc has two main components: a weakly-supervised temporal action localization (WSTAL) base model (Subsection 3.1) and an iterative refinement process (Subsection 3.2). Based on a trained WSTAL model, we generate pseudo foreground-background ground truth labels. We use these pseudo labels to supervise the training of a new WSTAL model. We repeat the process for  $\eta$  iterations to progressively improve the pseudo ground truth and refine the final action prediction segments. Figure 2 illustrates our RefineLoc approach.

### 3.1. WSTAL: Weakly-Supervised Temporal Action Localization Base Model

The input to WSTAL is an untrimmed video, while the output is temporal action segment predictions. First, WSTAL extracts features from  $T$  non-overlapping snippets, which are then fed into both a snippet-level action classifier and a background-foreground attention module. Then,

WSTAL combines the class activation and attention maps to produce a video label prediction  $\hat{\mathbf{y}}$ . During training, we supervise WSTAL with a cross-entropy loss between the ground truth video label  $\mathbf{y}$  and the predicted label  $\hat{\mathbf{y}}$ . Finally, we post-process the learned class activation and attention maps to produce action segment predictions. In what follows, we discuss the details of each module in WSTAL.

**Feature Extraction Module.** In order to compare with other works, we use two main feature extractor backbones: TSN [59] and I3D [9]. TSN is pretrained by UntrimmedNets [58] and used by multiple state-of-the-art works [33, 49, 64]. I3D is pretrained on Kinetics [26] and used as a feature extractor by several weakly-supervised methods [35, 37, 38, 42, 64]. We split the input untrimmed video into  $T$  non-overlapping  $H$ -frame-long clip snippets (15 for TSN and 16 for I3D). We transform each snippet into a 2048-dimensional feature vector by concatenating the two 1024-dimensional activation vectors from each stream’s global pooling layer (RGB and Optical Flow). This module final output is a  $T \times 2048$  feature map  $\mathbf{F}$ .

**Snippet-Level Classification Module.** This module receives the feature map  $\mathbf{F}$  and produces a  $T \times N$  class activation map  $\mathbf{C}$ , where  $N$  is the number of action classes (100 classes in ActivityNet v1.2 [6] and 20 in THUMOS14 [24]). It consists of a multi-layer perceptron (MLP) with  $L$  Fully-Connected (FC) layers interleaved with a ReLU activation function. We reduce the size of each hidden layer by 2, which makes the last layer of size  $\frac{2048}{2^{L-1}} \times N$ .

**Foreground-Background Attention Module.** The objective of this module is to learn a foreground attention weight for each snippet to suppress the background snippets activation and to focus mainly on foreground snippets. It transforms  $\mathbf{F}$  into a  $T \times 2$  foreground attention map  $\mathbf{A}$ . Similar to the Snippet-Level Classification Module, it consists of a MLP with  $L$  FC layers interleaved with a ReLU activation function. Each hidden layer size is reduced by a factor of 2, making the last FC layer of size  $\frac{2048}{2^{L-1}} \times 2$ .

Other weakly-supervised action localization methods, such as UntrimmedNets [58], employ an attention module to train their models. While we share a similar motivation, our attention module is different from theirs in one key aspect: their attention module is only supervised by the video-level label for the purpose of achieving a better video label accuracy, while our foreground attention is supervised by both the video-level label and a set of pseudo background-foreground labels with the goal of improving segment localization predictions. Refer to Subsection 3.2 for the pseudo ground truth label generation process.

**Video Label Prediction Module.** This module combines the information from  $\mathbf{C}$  and  $\mathbf{A}$  to generate an  $N$ -dimensional action class probability vector  $\hat{\mathbf{y}}$  for the video label. Specifically, we pass  $\mathbf{C}$  through a softmax layer across the class dimension to get  $\hat{\mathbf{C}}$ . Previous meth-

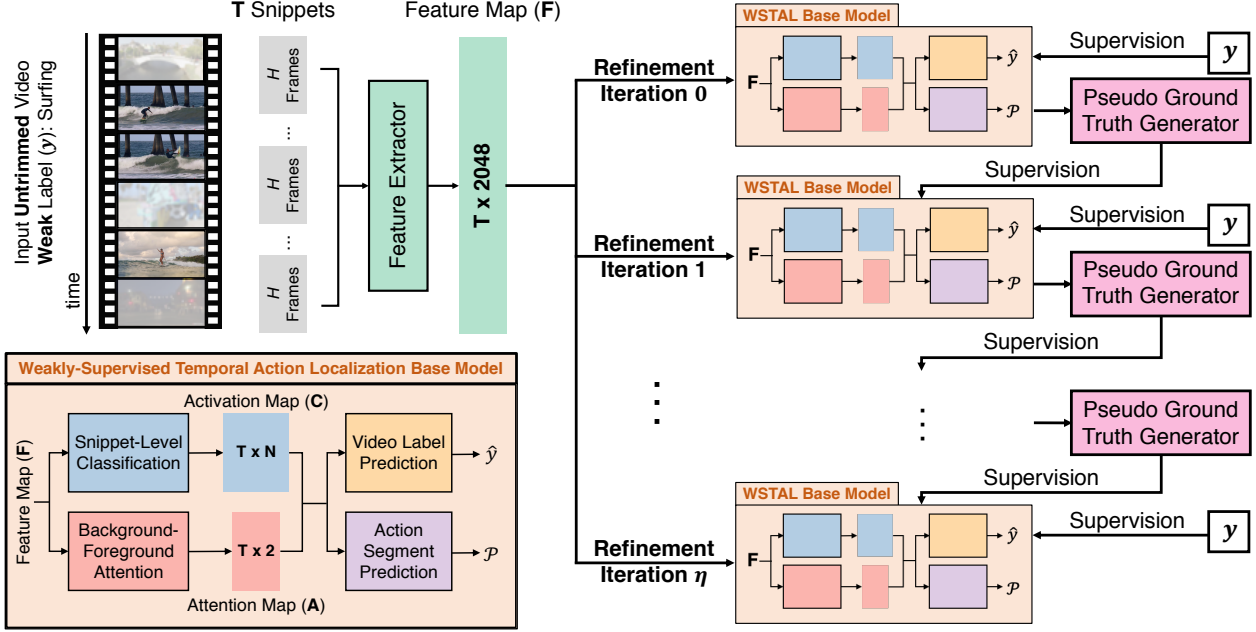


Figure 2: **Overview of RefineLoc Architecture.** Given an untrimmed video with only a weak label  $\mathbf{y}$ , we extract spatio-temporal features from  $T$  non-overlapping  $H$ -frame-long snippets (*top left*). We feed the  $T \times 2048$  features to an iterative refinement process (*right*). At each iteration, the feature map passes through our WSTAL base model (*bottom left*). WSTAL computes a snippet-level activation map ( $\mathbf{C}$ ) and a background-foreground attention map ( $\mathbf{A}$ ). Both  $\mathbf{A}$  and  $\mathbf{C}$  are used to predict the video label  $\hat{\mathbf{y}}$  and later to produce action segment predictions  $\mathcal{P}$ . At iteration 0, the pipeline is supervised using only  $\mathbf{y}$ . Subsequent iterations use both  $\mathbf{y}$  and pseudo ground truth generated from  $\mathbf{A}$  and  $\mathbf{C}$  of the previous iteration. We show in our experiments temporal action localization performance is improved after  $\eta$  iterations.

ods, have used one scalar to learn either class agnostic [33, 37, 38, 49, 58] or class specific [35] attention. However, since our method uses supervision directly on the attention values, we model the attention explicitly with two values, one for foreground and one for background. Thus, instead of learning the attention with a logistic-regression loss, we learn it as a binary classification problem. For doing so, we pass  $\mathbf{A}$  through two softmax layers. The first softmax layer operates across the foreground-background dimension to produce  $\bar{\mathbf{A}}^{bf}$ . The second softmax layer takes  $\bar{\mathbf{A}}^{bf}$  and operates across the time dimension (across snippets) to produce  $\bar{\mathbf{A}}^{time}$  as follows:

$$\bar{\mathbf{A}}_{t,i}^{bf} = \frac{\exp(\mathbf{A}_{t,i})}{\exp(\mathbf{A}_{t,1}) + \exp(\mathbf{A}_{t,2})}, \quad (1)$$

$$\bar{\mathbf{A}}_{t,i}^{time} = \frac{\exp(\bar{\mathbf{A}}_{t,i}^{bf})}{\sum_{t'=1}^T \exp(\bar{\mathbf{A}}_{t',i}^{bf})}. \quad (2)$$

Here, we use  $\bar{\mathbf{A}}^{bf}$  as the network’s predictions for the snippet-level foreground-background pseudo ground truth supervision (Subsection 3.2). Note that in Equations 1 and 2,  $i = 1$  refers to background while  $i = 2$  refers to foreground. Finally, we use  $\bar{\mathbf{A}}^{time}$  to weight sum the class activation map  $\bar{\mathbf{C}}$  when computing the video-label prediction

$\hat{\mathbf{y}} = \sum_{t=1}^T (\bar{\mathbf{A}}_{t,2}^{time} \cdot \bar{\mathbf{C}}_t)$ , where  $\bar{\mathbf{A}}_t$  and  $\bar{\mathbf{C}}_t$  are the foreground attention value and class activation vector of the  $t^{\text{th}}$  snippet. The way we compute  $\hat{\mathbf{y}}$  employs a soft attention mechanism that gives more weight to the class activation vectors of snippets with higher foreground attention values.

**Action Segment Prediction Module.** This module post-processes  $\bar{\mathbf{A}}$  and  $\bar{\mathbf{C}}$  to produce a set of action segment predictions  $\mathcal{P}$ . First, we remove background by filtering out snippets for which the background attention value is greater than a threshold  $\alpha_A$ . For each action class  $n$  from the top- $k$  classes in the predicted label  $\hat{\mathbf{y}}$ , we filter out any snippet  $t$ , whose classification score for that class  $\bar{\mathbf{C}}_{t,n}$  is lower than a threshold  $\alpha_C$ . Then, for each  $n$  class, we generate contiguous segments by grouping snippets that are separated by at most one filtered-out (background) snippet. We do so to overcome noise in the filtering process and connect segments that are close to each other. This process can be done in other and more sophisticated ways, however we keep the simplicity of the base model and rely mainly on our iterative process. We assign to each predicted segment  $(t_1, t_2)$  the label  $n$  and the score  $s$ ,

$$s = \frac{1}{t_2 - t_1 + 1} \sum_{t=t_1}^{t_2} (\bar{\mathbf{A}}_t^{time} + \bar{\mathbf{C}}_{t,n}) + \hat{\mathbf{y}}_n. \quad (3)$$

where  $\hat{y}_n$  is the video-level predictions score for the  $n^{\text{th}}$  class. Note that each prediction that comes from the  $n^{\text{th}}$  top- $k$  labels, has a different score  $s$ . Finally, to encode temporal context and deal with the ambiguity of action boundaries [1, 51], we inflate segments by 2 snippets at both ends.

### 3.2. Iterative Refinement Process

Let  $\mathcal{M}_0$  be the WSTAL base model trained using the weak video labels only. We iteratively refine this base model and its action predictions by introducing supervision on the background-foreground attention module using snippet-level pseudo ground truth labels. Let  $\mathcal{G}^{\mathcal{M}_\eta}$  be the pseudo ground truth generation function that uses information from  $\mathcal{M}_\eta$  (the trained WSTAL base model after iteration  $\eta$ ) to map each snippet to a pseudo foreground-background label. At iteration  $\eta+1$ , we train a new WSTAL base model  $\mathcal{M}_{\eta+1}$  on the joint loss for the weak video label and the snippet-level pseudo ground truth labels from  $\mathcal{G}^{\mathcal{M}_\eta}$ . Specifically, we compute the loss for  $\mathcal{M}_{\eta+1}$  on a given video in the following way,

$$\text{loss} = \mathcal{L}(\hat{\mathbf{y}}, \mathbf{y}) + \beta \frac{1}{T} \sum_{t=1}^T \mathcal{L}(\bar{\mathbf{A}}_t^{bf}, \mathcal{G}^{\mathcal{M}_\eta}(t)), \quad (4)$$

where  $\mathcal{L}$  is the cross-entropy loss and  $\beta$  is a trade-off coefficient to balance the loss signal of the pseudo ground truth with that of the video label. Note that the second cross-entropy loss is class-weighted to alleviate the imbalance in background and foreground pseudo labels.

**Pseudo Ground Truth Generation.** Intuitively, to obtain the maximum gain from the iterative refinement process, we want a pseudo ground truth generator that provides the closest approximation to the *true* snippet-level foreground-background ground truth labels, *i.e.* it should minimize the mislabelling rate. In order to overcome the possible bias learned by the pseudo ground truth generator process, and inspired by Hide and Seek [28], we only fixate on a portion of the pseudo ground truth at every iteration. We call this process *pseudo ground truth sampling* in which after every iteration, we only keep a percentage  $S$  of the generated pseudo ground truth, to use it as supervision in the next iteration. Here, we consider five different pseudo ground truth generation strategies. However the method is not constrained to use any specific type of generator, for instance other generator could be proposed to make the whole pipeline end-to-end. We study each generator’s effect on the final localization performance in Subsection 4.4.

**Uniformly Random Generator.** This generator assigns to each snippet a uniformly random pseudo label.

**Distribution Aware Generator.** Given a snippet, this generator produces, with a biased probability, a random pseudo ground truth label. The biased probability is equal to the average ratio of ground truth foreground to background

snippets in a video. This generator relies on information (namely the ratio) that requires access to temporal annotations. Thus, using such a generator does not align with the weakly-supervised setting, but we include it only as a baseline reference and we do not use it in our final model.

**Class Activation-Based Generator.** This generator selects the pseudo ground truth label for a snippet  $t$  by thresholding its maximum class score,  $\max(\bar{\mathbf{C}}_t)$ .

**Attention-Based Generator.** This generator produces the pseudo ground truth label for a snippet  $t$  by thresholding its foreground attention value,  $\bar{\mathbf{A}}_{t,2}^{time}$ .

**Segment Prediction-Based Generator.** This generator assigns pseudo labels based on the set of prediction segments  $\mathcal{P}$  produced by WSTAL. A snippet is given a pseudo foreground label if it is covered by a segment prediction, or given a pseudo background label otherwise. We use this generator in our final model due to its attractive performance gain as shown in the ablation in Subsection 4.4.

## 4. Experiments

We evaluate RefineLoc on two standard action localization benchmarks. First, we introduce the two datasets and the evaluation metric. Then, we give the implementation details for our RefineLoc model, including hyper-parameter values and training procedure details. Then, we compare our RefineLoc against state-of-the-art weakly supervised action localization methods using both TSN and I3D as our feature extractors. Subsequently, we present extensive ablation studies of our model, where we study the different pseudo ground truth generation strategies. Finally, we show some qualitative results of the temporal localization.

### 4.1. Datasets and Evaluation Metric

We conduct our experiments on ActivityNet v1.2 [6] and THUMOS14 [24] datasets. These datasets consist of untrimmed videos with (weak) video-level action labels. Both datasets already have temporal annotations for the start and the end of action instances. However, we discard these strong temporal labels during training.

**THUMOS14 [24].** This dataset has 1010 validation and 1574 testing videos annotated with 101 action classes at the video-level. Among these videos, only 200 validation and 213 testing videos have temporal annotations for only 20 action classes, which are limited to sport actions. As in prior work [19, 67], we only consider the 20 classes and use the 200 validation videos to train RefineLoc and the 213 testing videos to evaluate performance.

**ActivityNet v1.2 [6].** ActivityNet v1.2 comprises a total of 9682 untrimmed videos annotated with 100 activity classes. This dataset is officially split into training, validation, and testing subsets, where the testing subset labels are withheld for the annual challenge. Following other methods [42, 49],

we use the training subset (4819 videos) to train RefineLoc and the validation subset (2383 videos) to test the performance of our model. ActivityNet is the most challenging dataset due to its large-scale nature and, unlike THUMOS14, its diverse activity classes that range from household activities to sport actions.

**Evaluation Metric.** Following the evaluation convention traditionally established for temporal action localization, we compare RefineLoc against other methods according to mean Average Precision (mAP) and penalize duplicate detections. We report mAP at multiple temporal Intersection-over-Union (tIoU) thresholds and take the average mAP across tIoU thresholds 0.5:0.05:0.95 as the main metric for ActivityNet v1.2, while we consider the mAP at tIoU threshold 0.5 as the evaluation metric for THUMOS14.

## 4.2. Implementation Details

We extract features from two different architectures: an I3D model [9], and the same pre-trained TSN [59] model used in AutoLoc [49], with 16 and 15 number of frames per snippet ( $H$ ), respectively. Regarding our snippet-level classification and background-foreground attention modules, we choose  $L = 2$  FC layers for both, on ActivityNet and THUMOS14. Comparisons between learning a scalar attention through logistic regression and our proposed two dimensional attention can be found in **supplementary material**. In the action segment prediction module, we set the thresholds ( $\alpha_A, \alpha_C$ ) to (0.5, 0.005), respectively for ActivityNet, and to (0.5, 0.35) respectively for THUMOS14. We consider the top-2 labels when generating segment predictions in both datasets. After every iteration we randomly sample 80% of the pseudo ground truth ( $S = 80\%$ ). Finally, during training, we use an initial learning rate of  $10^{-4}$  and  $10^{-3}$  for ActivityNet and THUMOS14 experiments, respectively. We employ a learning rate exponential decay with a 0.9 decay factor. We train for a max of 50 epochs per refinement iteration and pick the best model from the epoch with the lowest validation loss from Equation 4.

## 4.3. State-of-the-Art Comparison

We compare our model to the state-of-the-art in temporal action localization, including weakly-supervised and fully-supervised methods. We show the comparison on both ActivityNet v1.2 and THUMOS14 datasets.

Table 1 summarizes results on ActivityNet v1.2, where we report mAP across different tIoU thresholds. After three refinement iterations, *i.e.* RefineLoc ( $\eta = 3$ ), the performance of our baseline model, *i.e.* RefineLoc ( $\eta = 0$ ), is significantly boosted by 13.6% in average mAP. For each tIoU, we observe that RefineLoc ( $\eta = 3$ ) improves upon previous methods by significant margins. For instance, we outperform CleanNet [33], the current state-of-the-art, by 1.5% in Avg. mAP. Lastly, the performance of our weakly-

Supervision	Model	Feats	0.5	0.75	0.95	Avg.
Full	Zhao <i>et al.</i> [67]	-	-	-	-	<b>25.9</b>
Weak	UntNets [58]	TSN	7.4	3.2	0.7	3.6
	AutoLoc [49]		27.3	15.1	3.3	16.0
	TSM [64]		28.3	17.0	3.5	17.1
	W-TALC [42]	I3D	37.0	-	-	18.0
	CleanNet [33]		37.1	20.3	5.0	21.6
	3C-Net [42]		35.4	-	-	21.1
	3C-Net† [42]		37.2	-	-	21.7
	<b>RefineLoc (Ours)</b>	TSN	<b>38.8</b>	22.2	5.3	<b>23.2</b>
<b>RefineLoc (Ours)</b>	I3D	38.7	<b>22.6</b>	<b>5.5</b>	<b>23.2</b>	

Table 1: **Results on ActivityNet v1.2.** We compare RefineLoc with state-of-the-art methods on ActivityNet v1.2, including weakly supervised methods and state-of-the-art fully supervised one, for reference. RefineLoc results were obtained using the Segment Prediction pseudo ground truth generation strategy with  $\beta = 4$ . RefineLoc outperforms other weakly supervised methods, and gets very close to state-of-the-art fully supervised performance on this challenging large-scale benchmark. 3C-Net† [35] uses number of instances per video as extra supervision.

Supervision	Model	Feats	0.3	0.5	0.7
Full	BMN [31]		56.0	38.8	20.5
	P-GCN [65]		<b>63.6</b>	<b>49.1</b>	-
Weak	UntNets [58]	TSN	28.2	13.7	-
	W-TALC [42]		32.0	18.8	6.2
	AutoLoc [49]		35.8	21.2	5.8
	TSM [64]		37.3	21.9	6.0
	STPN [37]	I3D	31.1	16.2	5.1
	W-TALC [42]		40.1	22.8	7.6
	TSM [64]		39.5	24.5	7.1
	3C-Net [42]		40.9	24.6	7.7
	3C-Net† [42]		44.2	26.6	8.1
	Nguyen <i>et al.</i> [38]		<b>46.6</b>	<b>26.8</b>	<b>9.0</b>
	<b>RefineLoc (Ours)</b>		TSN	36.1	22.6
<b>RefineLoc (Ours)</b>	I3D	40.8	23.1	5.3	

Table 2: **Results on THUMOS14.** We compare RefineLoc results with state-of-the-art methods (weakly and fully supervised) on THUMOS14. We note that the main metric for this dataset is mAP at tIoU threshold 0.5. Note that 3C-Net† [35] uses number of instances per video as extra supervision.

supervised model, which does not use any temporal action annotations in training, is only 2.7% behind the fully-supervised state-of-the-art [67] on this challenging benchmark. We attribute the effectiveness of our approach to its ability to supervise a foreground-background attention model via pseudo ground-truth, which results in overall tighter localization with less background errors.

For THUMOS14, we report results in Table 2. RefineLoc exhibits competitive performance to state-of-the-art methods [35, 38, 64], which use I3D as their feature extraction backbone. When RefineLoc is compared to the methods that use the TSN features, it achieves better mAP per-

formance compared with the best of them [64]. We observe again that refinement enhances our baseline model, *i.e.* RefineLoc ( $\eta = 0$ ), in this dataset by 14.77% mAP.

We show that our method is simple, yet effective. We demonstrate that the key component of RefineLoc is the iterative process, boosting results of the base model up to 13.6% points in average mAP for ActivityNet, and up to 14.8% in mAP at 0.5 IoU on THUMOS14. Despite its simplicity, RefineLoc outperforms all other methods using TSN features on THUMOS14, and beat the state-of-the-art on the most challenging dataset ActivityNet.

#### 4.4. Ablation Study

In this section, we present multiple ablation studies motivating the design choices for our RefineLoc approach. First, we study the performance of several pseudo ground truth generators and the influence of the loss trade-off coefficient  $\beta$  (Equation 4) on the performance of each generator. Afterwards, we analyze how our model’s performance changes from one refinement iteration to the next. Finally, we present a diagnosis study (using the DETAD [1] diagnostic tool) of the detection results before and after our iterative refinement process. We present all the studies in this subsection using ActivityNet v1.2 [6] dataset along with I3D features. For all the experiments in this section we report average mAP at tIoU thresholds 0.5:0.05:0.95. Refer to the **supplementary material** for the analysis of ActivityNet v1.2 using TSN features, and THUMOS14 [24] analysis.

**Effects of the Pseudo Ground Truth Generator and the Loss Trade-off Coefficient  $\beta$ .** Table 3 summarizes the best average mAP performance for the five pseudo ground truth generators and for five different values of  $\beta$ . The baseline model  $\mathcal{M}_0$  ( $\beta = 0$ ) achieves 9.66% average mAP at tIoU thresholds 0.5:0.05:0.95. Across all generator types and  $\beta$  values, we can see a performance improvement over  $\mathcal{M}_0$ . This shows the effectiveness of the iterative refinement process we propose. We can also conclude that the Segment Prediction-Based Generator gives the best performance gain compared to the other generators, mainly because this generator has access to information from both the class activation and attention maps. Moreover,  $\beta = 4$  strikes the best balance between the video label loss and the background-foreground pseudo ground truth loss. We observe similar behavior on THUMOS14 as well, *i.e.* the best generator is the segment prediction-based one, while the best  $\beta$  is 4.

**Performance over Refinement Iterations.** Table 4 shows the evolution of RefineLoc’s performance across five refinement iterations. We obtain the highest performance after  $\eta = 3$  iterations by achieving an average mAP of 23.24%. This is a significant 10.28% increase over our baseline model  $\mathcal{M}_0$  (refinement iteration 0 in the table). We can also see that one iteration of refinement boosts the results up to 9.48%. This clearly shows the effectiveness of lever-

Pseudo Ground Truth Generator	$\beta$					
	0	1	2	4	8	16
Uniform Random	—	9.66	9.66	9.66	9.66	9.66
Distribution Aware	—	17.39	19.10	20.00	17.73	18.30
Class Activation	—	23.09	23.02	22.93	22.86	22.85
Attention	—	<b>23.15</b>	23.13	22.97	23.00	22.94
Segment Prediction	—	23.04	<b>23.15</b>	<u>23.24</u>	<b>23.11</b>	<b>23.09</b>

Table 3: **Effects of pseudo ground truth generator and loss trade-off coefficient  $\beta$  in ActivityNet v1.2.** We summarize the performances of different pseudo label generators and the effect of the coefficient  $\beta$ . The segment prediction-based generator with  $\beta = 4$  shows the highest performance (underlined number). Bold numbers represent the best performing generator for a given  $\beta$ .

Refinement Iteration	0	1	2	3	4	5
<b>RefineLoc</b>	9.6	19.14	22.66	<b>23.24</b>	22.94	22.95

Table 4: **Effects of refinement.** We show the gain from iterative refinement on ActivityNet v1.2. We clearly see the improvement of segment prediction over iterations: 13.58% in 3 iterations.

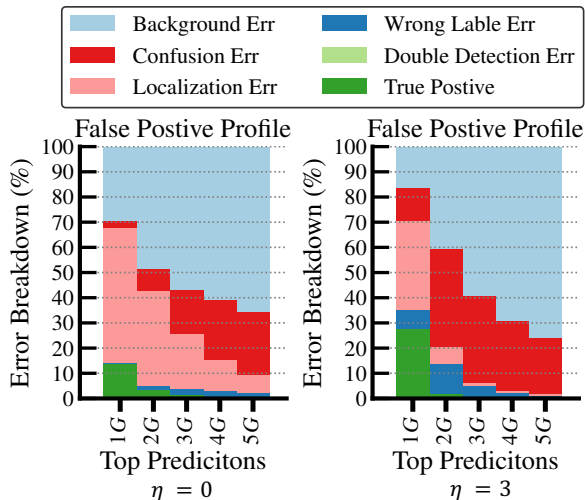


Figure 3: **Diagnosing Detection Results.** We present DETAD [1] false positive profiles of RefineLoc at refinement iterations 0 and 3.  $G$  represents the number of ground truth segments available in the ActivityNet dataset. Our refinement strategy clearly pushes more true positive predictions to the top  $1G$  scoring predictions. RefineLoc also reduces background and localization error at later iterations, indicating temporally tighter predictions.

aging the pseudo ground truth labels during training. We observe similar behavior in THUMOS14, where the best performance is achieved after  $\eta = 3$  refinement iterations.

**Diagnosing Detection Results.** To analyze the merits of the proposed refinement strategy, we conduct a DETAD [1] false-positive analysis of RefineLoc at refinement iterations 0 and 3. We present the results in Figure 3. The false-positive profile analysis provides a fine-grained categorization of false-positive errors and summarizes the distribution

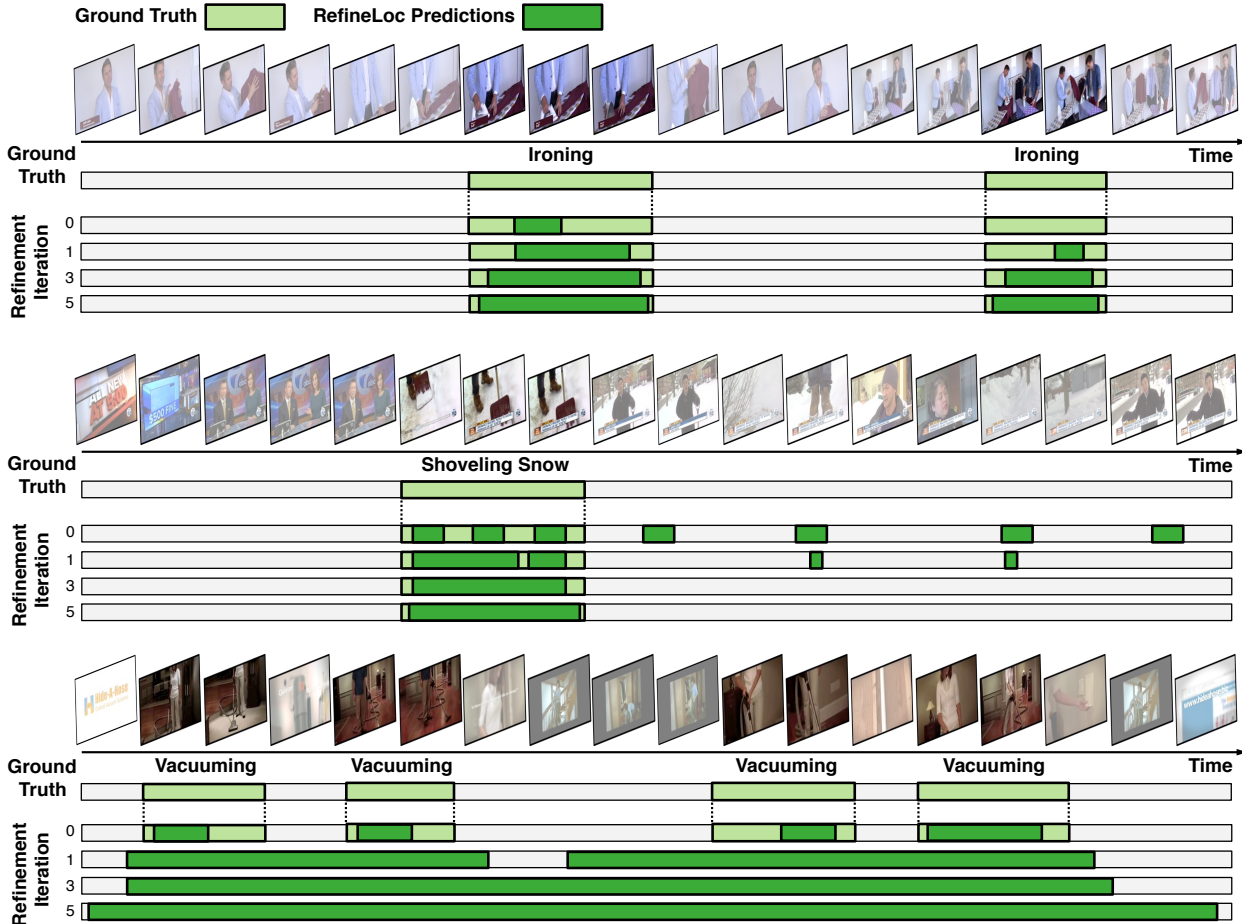


Figure 4: **Qualitative Results.** *Top:* RefineLoc successfully enhances prediction coverage over iterations and is able to detect missed instances as iterations evolve. *Middle:* RefineLoc manages to merge disjoint predictions and is also able to remove wrong background predictions from one iteration to the next. *Bottom:* In the presence of large context, iterative refinement can hurt RefineLoc predictions, as visual similarity between foreground and background confuses our attention model.

of these errors over the top 5 $G$  model predictions, where  $G$  is the number of ground truth segments in the dataset. After refinement (right plot), we observe that RefineLoc generates more high-scoring true positive predictions (towards 1 $G$ ). Despite the reduction of background and localization errors, there is an increase in confusion errors. We explain this increase due to the simplicity of our initial classification module. Besides, the extra supervision generated by the pseudo-ground truth encourage the model to improve the localization but not directly the label prediction.

#### 4.5. Qualitative Results

Figure 4 shows some RefineLoc qualitative detection results on ActivityNet. We present results for three different videos across different refinement iterations. The top video shows our method not only enhances its coverage over iterations, but is also able to detect a new instance at iteration 1 that was missed in the previous iteration. In the

middle video, we see how RefineLoc manages to successfully merge different predictions over iterations. We also see erroneous predictions being cut off from iteration to iteration. The final example shows a failure case. Despite starting with decent predictions at iteration 0, our predictions diverge drastically in subsequent steps.

## 5. Conclusions

In this work, we present RefineLoc, a novel weakly-supervised temporal action localization method. RefineLoc uses an iterative refinement strategy, where snippet-level pseudo labels are generated and used at every training iteration. Experiments show that RefineLoc outperforms the state-of-the-art on ActivityNet by 1.5% in average mAP. As labelling videos for action localization is a massive time and cost bottleneck, RefineLoc takes a step closer to alleviating the need for these prohibitively expensive tasks.



## References

- [1] Humam Alwassel, Fabian Caba Heilbron, Victor Escorcia, and Bernard Ghanem. Diagnosing error in temporal action detectors. In *ECCV*, 2018. 3, 5, 7, 11, 12
- [2] Hakan Bilen and Andrea Vedaldi. Weakly supervised deep detection networks. In *CVPR*, 2016. 3
- [3] Piotr Bojanowski, Rémi Lajugie, Francis Bach, Ivan Laptev, Jean Ponce, Cordelia Schmid, and Josef Sivic. Weakly supervised action labeling in videos under ordering constraints. In *ECCV*, 2014. 3
- [4] Shyamal Buch, Victor Escorcia, Chuanqi Shen, Bernard Ghanem, and Juan Carlos Niebles. Sst: Single-stream temporal action proposals. In *CVPR*, 2017. 2
- [5] Fabian Caba Heilbron, Juan Carlos Niebles, and Bernard Ghanem. Fast temporal activity proposals for efficient detection of human actions in untrimmed videos. In *CVPR*, 2016. 2
- [6] Fabian Caba Heilbron, Victor Escorcia, Bernard Ghanem, and Juan Carlos Niebles. Activitynet: A large-scale video benchmark for human activity understanding. In *CVPR*, 2015. 3, 5, 7, 11
- [7] Mathilde Caron, Piotr Bojanowski, Armand Joulin, and Matthijs Douze. Deep clustering for unsupervised learning of visual features. In *ECCV*, pages 132–149, 2018. 3
- [8] Mathilde Caron, Piotr Bojanowski, Julien Mairal, and Armand Joulin. Unsupervised pre-training of image features on non-curated data. In *ICCV*, 2019. 3
- [9] Joao Carreira and Andrew Zisserman. Quo vadis, action recognition? a new model and the kinetics dataset. In *CVPR*, 2017. 2, 3, 6, 11
- [10] Chien-Yi Chang, De-An Huang, Yanan Sui, Li Fei-Fei, and Juan Carlos Niebles. D<sup>3</sup>tw: Discriminative differentiable dynamic time warping for weakly supervised action alignment and segmentation. In *CVPR*, 2019. 3
- [11] Yu-Wei Chao, Sudheendra Vijayanarasimhan, Bryan Seybold, David A Ross, Jia Deng, and Rahul Sukthankar. Rethinking the faster r-cnn architecture for temporal action localization. In *CVPR*, 2018. 2
- [12] Guilhem Chéron, Jean-Baptiste Alayrac, Ivan Laptev, and Cordelia Schmid. A flexible model for training action localization with varying levels of supervision. In *NeurIPS*, pages 942–953, 2018. 3
- [13] Xiyang Dai, Bharat Singh, Guyue Zhang, Larry S Davis, and Yan Qiu Chen. Temporal context network for activity localization in videos. In *ICCV*, 2017. 2
- [14] Li Ding and Chenliang Xu. Weakly-supervised action segmentation with iterative soft boundary assignment. In *CVPR*, pages 6508–6516, 2018. 3
- [15] Olivier Duchenne, Ivan Laptev, Josef Sivic, Francis Bach, and Jean Ponce. Automatic annotation of human actions in video. In *ICCV*, 2009. 3
- [16] Victor Escorcia, Cuong D Dao, Mihir Jain, Bernard Ghanem, and Cees Snoek. Guess where? actor-supervision for spatiotemporal action localization. *arXiv preprint arXiv:1804.01824*, 2018. 3
- [17] Adrien Gaidon, Zaid Harchaoui, and Cordelia Schmid. Temporal localization of actions with actoms. *IEEE transactions on pattern analysis and machine intelligence*, 35(11):2782–2795, 2013. 2
- [18] J Gall and J Abu Farha. Ms-tcn: Multi-stage temporal convolutional network for action segmentation. In *CVPR*, 2019. 2
- [19] Jiyang Gao, Kan Chen, and Ram Nevatia. Ctap: Complementary temporal action proposal generation. In *ECCV*, 2018. 2, 5
- [20] Jiyang Gao, Zhenheng Yang, Kan Chen, Chen Sun, and Ram Nevatia. Turn tap: Temporal unit regression network for temporal action proposals. In *ICCV*, 2017. 2
- [21] Bernard Ghanem, Juan Carlos Niebles, Cees Snoek, Fabian Caba Heilbron, Humam Alwassel, Victor Escorcia, Ranjay Khristna, Shyamal Buch, and Cuong Duc Dao. The activitynet large-scale activity recognition challenge 2018 summary. *arXiv preprint arXiv:1808.03766*, 2018. 2
- [22] De-An Huang, Shyamal Buch, Lucio Dery, Animesh Garg, Li Fei-Fei, and Juan Carlos Niebles. Finding “it”: Weakly-supervised reference-aware visual grounding in instructional videos. In *CVPR*, 2018. 3
- [23] De-An Huang, Li Fei-Fei, and Juan Carlos Niebles. Connectionist temporal modeling for weakly supervised action labeling. In *ECCV*, 2016. 3
- [24] Haroon Idrees, Amir R Zamir, Yu-Gang Jiang, Alex Gorban, Ivan Laptev, Rahul Sukthankar, and Mubarak Shah. The thumos challenge on action recognition for videos in the wild. *Computer Vision and Image Understanding*, 155:1–23, 2017. 3, 5, 7, 11
- [25] Andrej Karpathy, George Toderici, Sanketh Shetty, Thomas Leung, Rahul Sukthankar, and Li Fei-Fei. Large-scale video classification with convolutional neural networks. In *CVPR*, 2014. 2
- [26] Will Kay, Joao Carreira, Karen Simonyan, Brian Zhang, Chloe Hillier, Sudheendra Vijayanarasimhan, Fabio Viola, Tim Green, Trevor Back, Paul Natsev, et al. The kinetics human action video dataset. *arXiv preprint arXiv:1705.06950*, 2017. 2, 3
- [27] Hilde Kuehne, Alexander Richard, and Juergen Gall. Weakly supervised learning of actions from transcripts. *Computer Vision and Image Understanding*, pages 78–89, 2017. 3
- [28] Krishna Kumar Singh and Yong Jae Lee. Hide-and-seek: Forcing a network to be meticulous for weakly-supervised object and action localization. In *Proceedings of the IEEE International Conference on Computer Vision*, pages 3524–3533, 2017. 2, 5
- [29] Ivan Laptev. On space-time interest points. *International journal of computer vision*, 64(2-3):107–123, 2005. 2
- [30] Ivan Laptev, Marcin Marszalek, Cordelia Schmid, and Benjamin Rozenfeld. Learning realistic human actions from movies. In *CVPR*, pages 1–8, 2008. 3
- [31] Tianwei Lin, Xiao Liu, Xin Li, Errui Ding, and Shilei Wen. Bmn: Boundary-matching network for temporal action proposal generation. In *The IEEE International Conference on Computer Vision (ICCV)*, October 2019. 6
- [32] Tianwei Lin, Xu Zhao, Haisheng Su, Chongjing Wang, and Ming Yang. Bsn: Boundary sensitive network for temporal action proposal generation. In *ECCV*, 2018. 2
- [33] Ziyi Liu, Le Wang, Qilin Zhang, Zhaning Gao, Zhenxing Niu, Nanning Zheng, and Gang Hua. Weakly supervised temporal action localization through contrast based evaluation networks. In *Proceedings of the IEEE International*

- Conference on Computer Vision*, pages 3899–3908, 2019. 1, 2, 3, 4, 6
- [34] Antoine Miech, Jean-Baptiste Alayrac, Piotr Bojanowski, Ivan Laptev, and Josef Sivic. Learning from video and text via large-scale discriminative clustering. In *ICCV*, 2017. 3
- [35] Sanath Narayan, Hisham Cholakkal, Fahad Shahbaz Khan, and Ling Shao. 3c-net: Category count and center loss for weakly-supervised action localization. In *Proceedings of the IEEE International Conference on Computer Vision*, pages 8679–8687, 2019. 3, 4, 6
- [36] Natalia Neverova, James Thewlis, Riza Alp Guler, Iasonas Kokkinos, and Andrea Vedaldi. Slim densepose: Thrifty learning from sparse annotations and motion cues. In *CVPR*, pages 10915–10923, 2019. 3
- [37] Phuc Nguyen, Ting Liu, Gautam Prasad, and Bohyung Han. Weakly supervised action localization by sparse temporal pooling network. In *CVPR*, 2018. 1, 2, 3, 4, 6
- [38] Phuc Xuan Nguyen, Deva Ramanan, and Charless C Fowlkes. Weakly-supervised action localization with background modeling. In *Proceedings of the IEEE International Conference on Computer Vision*, pages 5502–5511, 2019. 3, 4, 6
- [39] Dan Oneata, Jakob Verbeek, and Cordelia Schmid. Efficient action localization with approximately normalized fisher vectors. In *CVPR*, 2014. 2
- [40] Maxime Oquab, Léon Bottou, Ivan Laptev, and Josef Sivic. Is object localization for free?-weakly-supervised learning with convolutional neural networks. In *CVPR*, 2015. 3
- [41] George Papandreou, Liang-Chieh Chen, Kevin P Murphy, and Alan L Yuille. Weakly-and semi-supervised learning of a deep convolutional network for semantic image segmentation. In *ICCV*, 2015. 3
- [42] Sujoy Paul, Sourya Roy, and Amit K Roy-Chowdhury. W-talc: Weakly-supervised temporal activity localization and classification. In *ECCV*, 2018. 1, 2, 3, 5, 6
- [43] AJ Piergiovanni and Michael S Ryoo. Learning latent super-events to detect multiple activities in videos. In *CVPR*, 2018. 2
- [44] Alexander Richard, Hilde Kuehne, and Juergen Gall. Weakly supervised action learning with rnn based fine-to-coarse modeling. In *CVPR*, 2017. 3
- [45] Alexander Richard, Hilde Kuehne, Ahsan Iqbal, and Juergen Gall. Neuralnetwork-viterbi: A framework for weakly supervised video learning. In *CVPR*, pages 7386–7395, 2018. 3
- [46] David Rolnick, Andreas Veit, Serge Belongie, and Nir Shavit. Deep learning is robust to massive label noise. *arXiv preprint arXiv:1705.10694*, 2017. 2
- [47] Miaoqing Shi, Holger Caesar, and Vittorio Ferrari. Weakly supervised object localization using things and stuff transfer. In *ICCV*, 2017. 3
- [48] Zheng Shou, Jonathan Chan, Alireza Zareian, Kazuyuki Miyazawa, and Shih-Fu Chang. Cdc: Convolutional-deconvolutional networks for precise temporal action localization in untrimmed videos. In *CVPR*, 2017. 2
- [49] Zheng Shou, Hang Gao, Lei Zhang, Kazuyuki Miyazawa, and Shih-Fu Chang. Autoloc: weakly-supervised temporal action localization in untrimmed videos. In *ECCV*, 2018. 1, 2, 3, 4, 5, 6
- [50] Zheng Shou, Dongang Wang, and Shih-Fu Chang. Temporal action localization in untrimmed videos via multi-stage cnns. In *CVPR*, 2016. 2
- [51] Gunnar A Sigurdsson, Olga Russakovsky, and Abhinav Gupta. What actions are needed for understanding human actions in videos? In *ICCV*, 2017. 5
- [52] Karen Simonyan and Andrew Zisserman. Two-stream convolutional networks for action recognition in videos. In *Advances in neural information processing systems*, 2014. 2
- [53] Krishna Kumar Singh and Yong Jae Lee. Hide-and-seek: Forcing a network to be meticulous for weakly-supervised object and action localization. In *ICCV*, 2017. 3
- [54] Khurram Soomro, Amir Roshan Zamir, and Mubarak Shah. Ucf101: A dataset of 101 human actions classes from videos in the wild. *arXiv preprint arXiv:1212.0402*, 2012. 2
- [55] Peng Tang, Xinggang Wang, Xiang Bai, and Wenyu Liu. Multiple instance detection network with online instance classifier refinement. In *CVPR*, 2017. 1, 3
- [56] Du Tran, Lubomir Bourdev, Rob Fergus, Lorenzo Torresani, and Manohar Paluri. Learning spatiotemporal features with 3d convolutional networks. In *ICCV*, 2015. 2
- [57] Heng Wang and Cordelia Schmid. Action recognition with improved trajectories. In *ICCV*, 2013. 2
- [58] Limin Wang, Yuanjun Xiong, Dahua Lin, and Luc Van Gool. Untrimmednets for weakly supervised action recognition and detection. In *CVPR*, 2017. 1, 2, 3, 4, 6
- [59] Limin Wang, Yuanjun Xiong, Zhe Wang, Yu Qiao, Dahua Lin, Xiaoou Tang, and Luc Van Gool. Temporal segment networks: Towards good practices for deep action recognition. In *ECCV*, 2016. 2, 3, 6, 11
- [60] Huijuan Xu, Abir Das, and Kate Saenko. R-c3d: Region convolutional 3d network for temporal activity detection. In *ICCV*, 2017. 2
- [61] Huijuan Xu, Kun He, Leonid Sigal, Stan Sclaroff, and Kate Saenko. Text-to-clip video retrieval with early fusion and re-captioning. 2019. 2
- [62] Jia Xu, Alexander G Schwing, and Raquel Urtasun. Learning to segment under various forms of weak supervision. In *CVPR*, 2015. 3
- [63] Serena Yeung, Olga Russakovsky, Greg Mori, and Li Fei-Fei. End-to-end learning of action detection from frame glimpses in videos. In *CVPR*, 2016. 2
- [64] Tan Yu, Zhou Ren, Yuncheng Li, Enxu Yan, Ning Xu, and Junsong Yuan. Temporal structure mining for weakly supervised action detection. In *Proceedings of the IEEE International Conference on Computer Vision*, pages 5522–5531, 2019. 3, 6, 7
- [65] Runhao Zeng, Wenbing Huang, Mingkui Tan, Yu Rong, Peilin Zhao, Junzhou Huang, and Chuang Gan. Graph convolutional networks for temporal action localization. In *The IEEE International Conference on Computer Vision (ICCV)*, October 2019. 6
- [66] Yongqiang Zhang, Yancheng Bai, Mingli Ding, Yongqiang Li, and Bernard Ghanem. W2f: A weakly-supervised to fully-supervised framework for object detection. In *CVPR*, 2018. 1, 3
- [67] Yue Zhao, Yuanjun Xiong, Limin Wang, Zhirong Wu, Xiaoou Tang, and Dahua Lin. Temporal action detection with structured segment networks. In *ICCV*, 2017. 2, 5, 6

## Supplementary Material

### A. Additional Ablation Study

We include here the same ablation study presented in the main paper (Subsection 4.4) for three additional model settings: TSN [59] features on ActivityNet v1.2 [6], TSN and I3D [9] features on THUMOS14 [24].

**Effects of the Pseudo Ground Truth Generator and the Loss Trade-off Coefficient  $\beta$ .** Tables 5a, 5c, and 5b summarize the best performance for the five generators and for five different  $\beta$  values on ActivityNet v1.2 using TSN, THUMOS14 using I3D, and THUMOS14 using TSN, respectively. The Segment Prediction-Based Generator consistently gives the best performance gain compared to the other generators in all settings.

**Performance over Refinement Iterations.** Tables 6a, 6c, and 6b show the evolution of RefineLoc’s performance across refinement iterations on ActivityNet v1.2 using TSN, THUMOS14 using I3D, and THUMOS14 using TSN, respectively. In each setting, we consistently observe a significant performance increase over our baseline model  $\mathcal{M}_0$  (refinement iteration 0 in the table).

**Diagnosing Detection Results.** To further analyze the merits of the proposed refinement strategy, we conduct a DETAD [1] false positive analysis of RefineLoc on ActivityNet v1.2 using TSN, THUMOS14 using I3D, and THUMOS14 using TSN (Figures 5a, 5c, and 5b, respectively). After refinement (right plot in each figure), we observe that RefineLoc generates more high-scoring true positive predictions (towards 1G) and reduces background and localization errors. The DETAD results indicate that our iterative refinement encourages tighter temporal predictions, which we argue does occur primarily because of the snippet-level supervision injected in the form of pseudo ground truth.

### B. Logistic Regression vs Cross-Entropy

RefineLoc learns two values for the attention, instead of learning one single scalar. The motivation behind this design choice is to learn explicitly one value for background attention and one value for foreground attention. Besides, learning these two values through a classification loss (*i.e.* cross-entropy) is an easier problem than learning one value through a regression loss (*i.e.* logistic regression). For ActivityNet, we found that our initial hypothesis is true. Indeed, when we learn only one scalar for attention, RefineLoc obtains only 22.2% average mAP using I3D features, a 1% drop in average mAP compared to the results obtained with cross-entropy. In contrast, the best result on THUMOS14 is obtained by learning only one scalar value. When learning two values for attention with cross-entropy, our model obtains only 19.95% mAP at tIoU 0.5.

### C. Qualitative Results (THUMOS14)

Figure 6 showcases RefineLoc qualitative results from the THUMOS14 dataset. We present results for three different videos over different refinement iterations. The top video shows our method not only enhances its coverage over iterations, but is also able to detect a new instance at iteration 1 that was missed in the previous iteration. In the middle video, we see how RefineLoc manages to successfully cut off erroneous predictions from iteration to iteration. The final example shows a failure case. Despite starting with decent predictions at iteration 0, our predictions do not improve in subsequent steps. We believe this confusion comes from the heavy context around the actions.

Pseudo Ground Truth Generator	$\beta$					
	0	1	2	4	8	16
Uniform Random	13.15	13.15	13.15	13.15	13.15	13.15
Distribution Aware	15.27	19.22	18.76	20.80	20.96	20.96
Class Activation	22.95	22.90	22.53	22.55	22.23	22.23
Attention	<b>23.15</b>	22.90	22.47	22.57	22.36	22.36
Segment Prediction	23.09	<b>23.16</b>	<b>22.98</b>	<b>23.02</b>	<b>22.88</b>	<b>22.88</b>

(a) **ActivityNet v1.2 with TSN features.** The segment prediction-based generator with  $\beta = 2$  shows the highest performance (underlined number).

Pseudo Ground Truth Generator	$\beta$					
	0	1	2	4	8	16
Uniform Random	19.45	21.12	20.20	19.78	19.45	19.45
Distribution Aware	20.69	20.32	19.45	19.45	19.45	19.45
Class Activation	20.18	20.11	20.10	20.21	20.34	20.34
Attention	19.45	19.45	19.45	19.45	19.45	19.45
Segment Prediction	21.48	<b>22.60</b>	<b>21.55</b>	<b>20.85</b>	<b>21.09</b>	<b>21.09</b>

(b) **THUMOS14 with I3D features.** The segment prediction-based generator with  $\beta = 2$  shows the highest performance (underlined number).

Pseudo Ground Truth Generator	$\beta$					
	0	1	2	4	8	16
Uniform Random	2.90	17.97	17.64	18.60	18.96	16.64
Distribution Aware	14.89	14.73	14.90	16.42	14.50	14.50
Class Activation	12.12	12.32	13.66	12.98	13.28	13.28
Attention	20.70	21.37	21.10	20.64	19.66	19.66
Segment Prediction	<b>20.92</b>	<b>21.87</b>	<b>22.63</b>	<b>21.13</b>	<b>20.64</b>	<b>20.64</b>

(c) **THUMOS14 with TSN features.** The segment prediction-based generator with  $\beta = 4$  shows the highest performance (underlined number).

Table 5: **Effects of pseudo ground truth generator and loss trade-off coefficient  $\beta$ .** We summarize the performances of different pseudo label generators and the effect of the coefficient  $\beta$ . The reported metric is average mAP (at tIoU thresholds 0.5 : 0.05 : 0.95) for ActivityNet v1.2 and mAP at 0.5 tIoU threshold for THUMOS14. Bold numbers represent the best performing generator for a given  $\beta$ .

Refinement Iteration	0	1	2	3	4	5
<b>RefineLoc</b>	13.27	21.62	22.76	23.09	22.68	<b>23.23</b>

(a) **ActivityNet v1.2 using I3D features.** We observe a significant improvement of 9.96% in 5 iterations.

Refinement Iteration	0	3	6	9	12	14
<b>RefineLoc</b>	19.45	20.96	21.36	22.46	21.87	<b>23.12</b>

(b) **THUMOS14 using I3D features.** We observe a significant improvement of 3.67% after 14 iterations.

Refinement Iteration	0	1	2	3	4	5
<b>RefineLoc</b>	2.90	11.13	18.73	20.60	<b>22.63</b>	20.12

(c) **THUMOS14 using TSN features.** We observe a significant improvement of 19.73% after 4 iterations.

Table 6: **Performance over refinement iterations.** We show the gain from our proposed iterative refinement process. The reported metric is average mAP (at tIoU thresholds 0.5 : 0.05 : 0.95) for ActivityNet v1.2 and mAP at 0.5 tIoU threshold for THUMOS14. We observe that even with a weak base model, our method has the capability to improve the performance over iterations.

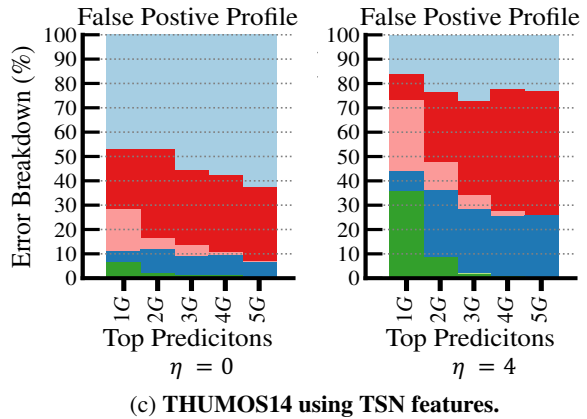
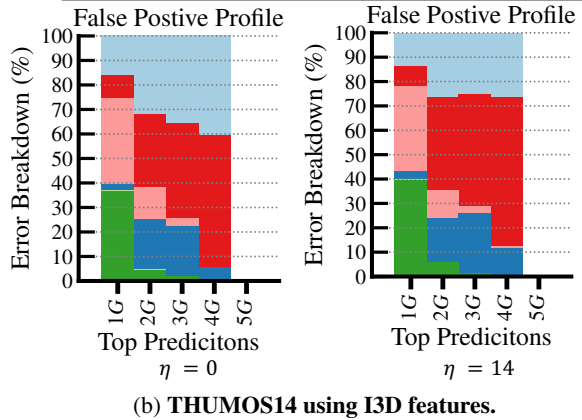
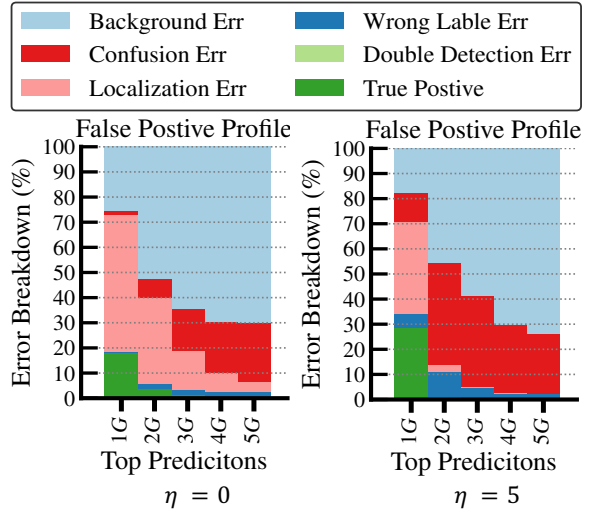


Figure 5: **Diagnosing Detection Results.** We present DETAD [1] false positive profiles of RefineLoc at refinement iterations  $\eta = 0$  (left) and  $\eta = \text{convergence}$  (right).  $G$  represents the number of ground truth segments available in the dataset.

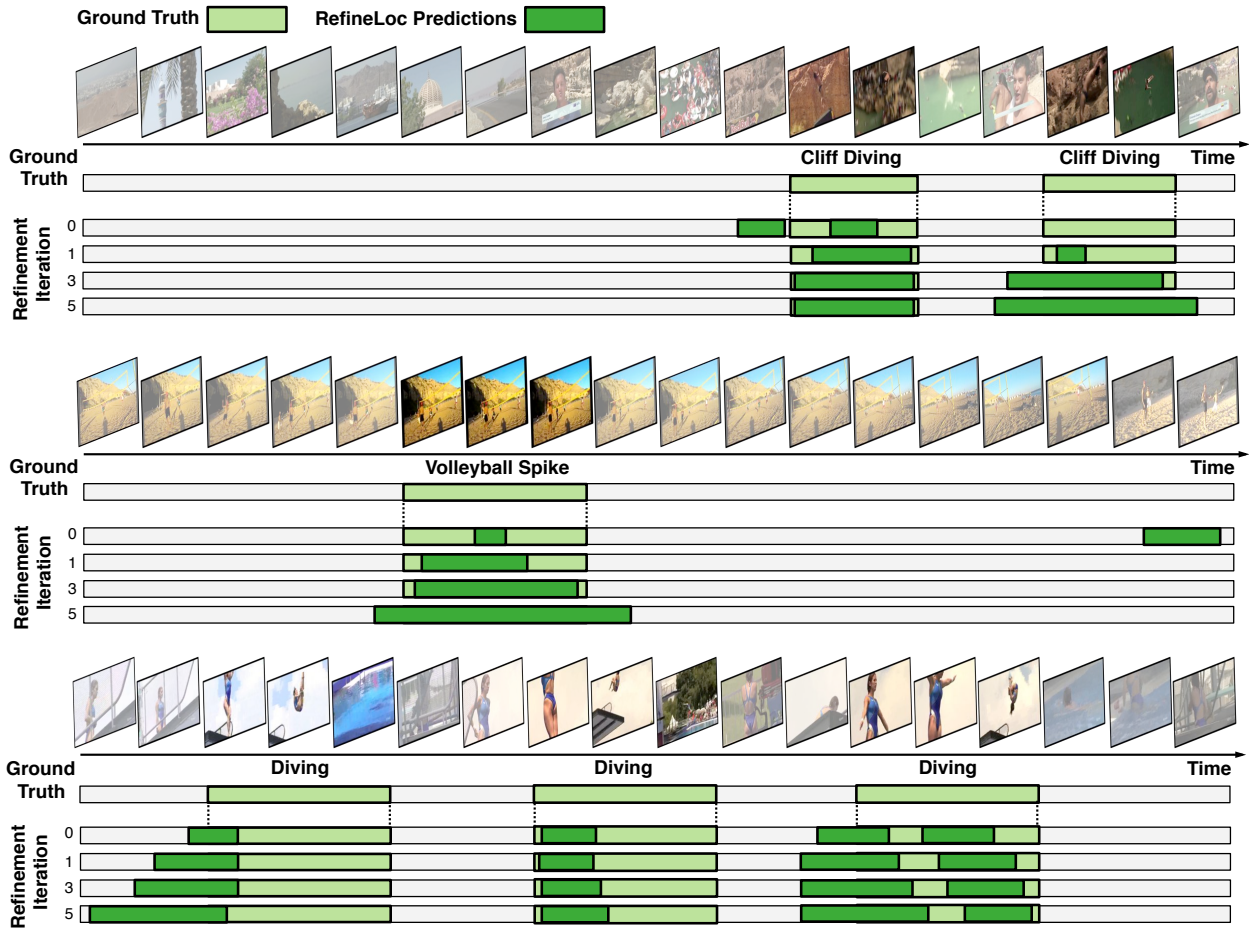


Figure 6: **Qualitative Results.** *Top and Middle:* RefineLoc successfully enhances prediction coverage over iterations and is able to detect missed instances as iterations evolve. *Bottom:* In the presence of large context, iterative refinement can hurt RefineLoc predictions, as visual similarity between foreground and background confuses our attention model.